RESEARCH ARTICLE | JANUARY 16 2018

Confined-path interference suppressed quantum correction on weak antilocalization effect in a $BiSbTeSe_2$ topological insulator

Lai-Xiang Qin; Xin-Chen Pan; Feng-Qi Song; Liang Zhang; Zhang-Hao Sun; Ming-Qiang Li; Peng Gao; Ben-Chuan Lin; Shiu-Ming Huang; Rui Zhu; Jun Xu; Fang Lin; Hai-Zhou Lu; Dapeng Yu; Zhi-Min Liao

Appl. Phys. Lett. 112, 032102 (2018)
https://doi.org/10.1063/1.5009507

Confined-path interference suppressed quantum correction on weak antilocalization effect in a $BiSbTeSe_2$ topological insulator

Lai-Xiang Qin,[1] Xin-Chen Pan,[2] Feng-Qi Song,[2] Liang Zhang,[1] Zhang-Hao Sun,[1] Ming-Qiang Li,[3] Peng Gao,[3,4,5] Ben-Chuan Lin,[1] Shiu-Ming Huang,[6] Rui Zhu,[3] Jun Xu,[3] Fang Lin,[1] Hai-Zhou Lu,[7] Dapeng Yu,[1,7] and Zhi-Min Liao[1,4,a)]

[1]*State Key Laboratory for Mesoscopic Physics, School of Physics, Peking University, Beijing 100871, People's Republic of China*
[2]*National Laboratory of Solid State Microstructures, Collaborative Innovation Center of Advanced Microstructures and School of Physics, Nanjing University, Nanjing 210093, People's Republic of China*
[3]*Electron Microscopy Laboratory, School of Physics, Peking University, Beijing 100871, People's Republic of China*
[4]*Collaborative Innovation Center of Quantum Matter, Beijing 100871, People's Republic of China*
[5]*International Center for Quantum Materials, School of Physics, Peking University, Beijing 100871, China*
[6]*Department of Physics, National Sun Yat-Sen University, Kaohsiung 80424, Taiwan*
[7]*Institute for Quantum Science and Engineering and Department of Physics, South University of Science and Technology of China, Shenzhen 518055, People's Republic of China*

(Received 17 October 2017; accepted 29 December 2017; published online 16 January 2018)

We have studied the magnetoconductance in a topological insulator $BiSbTeSe_2$ with different probe lengths. The magnetoconductance correction reduces by a factor of 2 when the probe length is comparable to the phase coherence length, L_φ, and the related weak antilocalization prefactor, α, reduces by a factor of 2. L_φ is independent of the probe length and follows the $T^{-0.5}$, corresponding to the two-dimensional electron-electron interaction. α shows similar back-gate voltage dependence and L_φ is almost the same in both short and long channels. This indicates that the widely reported surface-to-bulk coupling is not the dominant mechanism of the α reduction. Moreover, non-saturating magnetoresistances are observed and coincided with each other in the short and long channels. The reduced α is deemed to be due to the quantum correction effect caused by the geometries and electrode distribution. The finding here will further the understanding of the transport properties of the topological insulators and unveil exotic quantum phenomena. *Published by AIP Publishing.*
https://doi.org/10.1063/1.5009507

Three-dimensional (3D) topological insulators (TIs) possess insulating bulk and gapless surface states, which are protected by time reversal symmetry.[1–3] The existence of topological surface states has been confirmed through angle resolved photoemission spectroscopy (ARPES) and scanning tunneling microscopy (STM).[4–6] The carrier transport properties of the surface state are widely investigated through the weak-antilocalization (WAL) theory.[7–9] The underlying physical picture of WAL is that the Dirac fermions traveling along two time-reversed self-intersecting loops accumulate a π Berry phase, resulting in the destructive quantum interference. When a magnetic field is applied on the material, time reversal symmetry will be broken and the destructive quantum interference will be suppressed, leading to a magnetoconductance cusp in the zero magnetic field region.[10] Many experimental works reported the carrier characteristics extracted from WAL, and the values of the WAL prefactor α show wide range distribution. This range deviation is ascribed to different degrees of surface-to-bulk carrier coupling.[11–13] The transport of the topological surface states is robust to non-magnetic extrinsic impurities.[14–16] The carrier coherence length is as long as sub-micrometer that is comparable to the size of exfoliated topological insulator (TI) nanoflake systems.[17,18] Besides surface-to-bulk carrier coupling, this long coherence length might reach the WAL theory limit in the experimental conditions. This might challenge the fundamental concept and lead to the deviation of the "detected" characteristics.

The question arises as to that whether geometries as well as probe distributions play an important role in the quantum correction. The size confined effect on the transport characteristics has been investigated in nanowires.[15] However, it is still not clear what influence the probe distribution has on transport characteristics. In order to figure out this puzzle, we investigated the magnetoconductance of a TI single crystal with different detection channel lengths. To optimize the geometry probe effect and limit the widely discussed surface-to-bulk coupling, the $BiSbTeSe_2$ (BSTS) topological insulator, which is known as having extremely low bulk state contribution, is employed in this study.[14,16,19,20] The experimental results support that the observed magnetoconductance is obviously suppressed when the probed channel length is comparable to the electron coherence length.

The BSTS single crystals were grown by the method described elsewhere.[21] The as-grown crystal was cleaved along the basal plane with a silvery mirror-like surface. As shown in Fig. 1(a), the energy-dispersive X-ray spectroscopy (EDS) images performed in an aberration corrected scanning transmission electron microscope (TEM, FEI Titan Cubed Themis G2 300) indicate the high uniformity of the elemental distribution. The high-resolution TEM image [Fig. 1(b)] shows the equally spaced lattice fringes, indicating that the BSTS samples are high-quality single crystals. The

a)Email: liaozm@pku.edu.cn

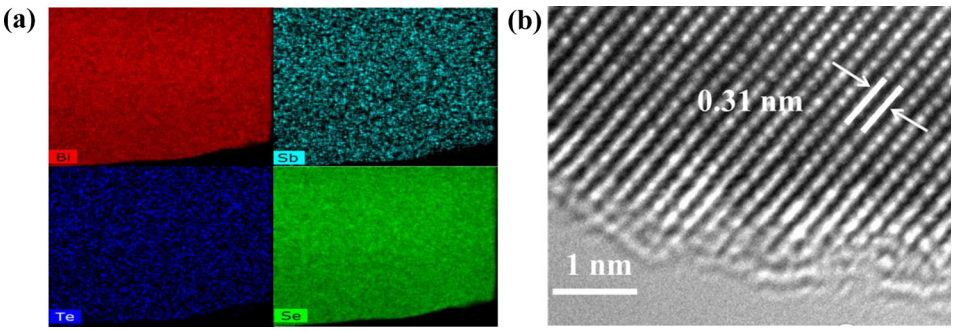

FIG. 1. (a) Elemental mapping of the BSTS single crystal. (b) The high resolution TEM image of the BSTS single crystal. The lattice spacing 0.31 nm corresponds to the (015) plane.

calculated lattice separation is 0.31 nm, corresponding to the (015) plane. The existence of the surface states of this BSTS topological insulator was confirmed by the half-quantum Hall effect.[21]

The BSTS flakes were mechanically exfoliated from the ingot crystal by the Scotch-tape and transferred onto Si substrates with 280 nm SiO_2. The standard electron-beam lithography technique is used to pattern the contact electrodes. The Cr (20 nm)/Au (150 nm) electrodes were deposited by the electron beam evaporation, and the electrode width is 1 μm. The transport measurements were performed by the standard lock-in techniques with a frequency of 17.777 Hz and a bias current of 0.1 μA. The Si substrate served as a back gate, and the resistance was measured by a 4-probe method. The measurement configuration is schematically illustrated in Fig. 2(a). The optical image of a typical device is shown in Fig. 2(b). The probed channel lengths are 1.5 μm (long length, electrodes 2 and 3) and 360 nm (short length, electrodes 3 and 4), respectively. The channel width is ~4.07 μm. Figure 2(c) shows the temperature dependence of the resistance measured from the short channel. The resistance increases as temperature decreases and reaches a maximum at 125 K and then decreases as temperature decreases below 125 K. This behavior could be understood by the two-source, surface and bulk, conductance contribution model. The bulk carriers are thermally excited at high temperatures. The thermal activation energy decreases as temperature decreases, leading to that the conductance contribution from the bulk state is gradually suppressed. The transport behavior is dominated by the surface states at low temperatures, and it is a metallic behavior.

Figures 3(a) and 3(b) show the conductivity correction, $\Delta\sigma(B) = \sigma(B) - \sigma(0)$, measured from the short and long channels, respectively. The conductivity correction of the short channel is half of that of the long channel at all temperatures. When a magnetic field is applied perpendicular to a two-dimensional system, it changes the interference of the electronic wave and leads to a conductance correction. The related conductivity correction can be expressed by the Hikami-Larkin-Nagaoka (HLN) model. As shown in Figs. 3(a) and 3(b), the data points fit well with the HLN formula,[8,10]

$$\Delta\sigma(B) = -\alpha \cdot \frac{e^2}{2\pi^2\hbar}\left[\Psi\left(\frac{1}{2}+\frac{B_\Phi}{B}\right) - \ln\left(\frac{B_\Phi}{B}\right)\right],$$

where $\Delta\sigma$ is the two-dimensional conductivity correction which is defined as $\Delta\sigma = \Delta G \cdot L/W$. L is the channel length and W is the width of the sample. Ψ is the digamma function and $B_\varphi = \hbar/4eL^2_\varphi$, where L_φ is the phase coherence length. α is related to the effective coherent transport channel in topological insulators. Theoretically, α is 0.5 for one independent coherence channel.[16] The coupling between different carrier transport channels would directly influence the value of α, which can be regarded as an indication for the degree of coupling strength.[22,23] It is also found that the conductance at 1.5 K [see Fig. 3(a)] shows oscillating behavior, which may originate from the coherence effect of the electronic waves from different paths, that is, the universal conductance fluctuations (UCF).

Figures 3(c) and 3(d) show the extracted α and L_φ as a function of temperature, respectively. The extracted L_φ values from the two probe channels are the same. It can be concluded from the inset in Fig. 3(d) that L_φ follows the relation of $T^{-0.46}$, which is in good agreement with the theoretical prediction of $T^{-0.5}$, for the electron-electron interaction in two dimensional systems.[23,24] This indicates that the observed magnetotransport behaviors are mainly from the two dimensional surface states of the BSTS topological insulator.[25] The consistent L_φ from the short and long channels supports that the carrier transport is highly uniform. α is roughly 0.4 for the long probe channel and that is very close to the theoretically predicted value, 0.5, for one conduction channel. α for the short probe channel is 0.2 and that is roughly half of the value in the long probe channel. Recent experiments reveal that α would be related to the disorder level and the estimated value is roughly 0.03,[26,27] which is much smaller than the observed α deviation here.

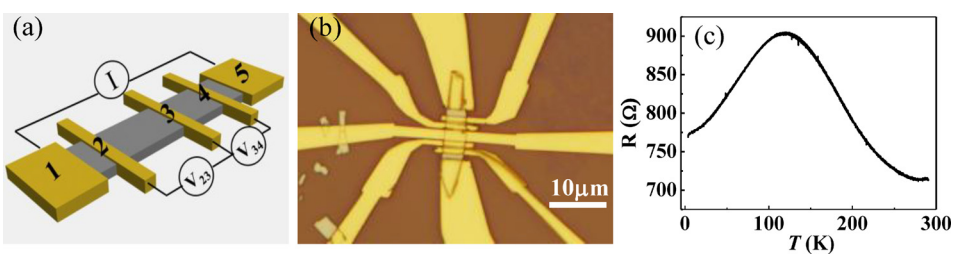

FIG. 2. (a) Schematic of the measurement configuration. (b) Optical image of a typical BSTS device. (c) Temperature dependence of resistance of the short probe channel device.

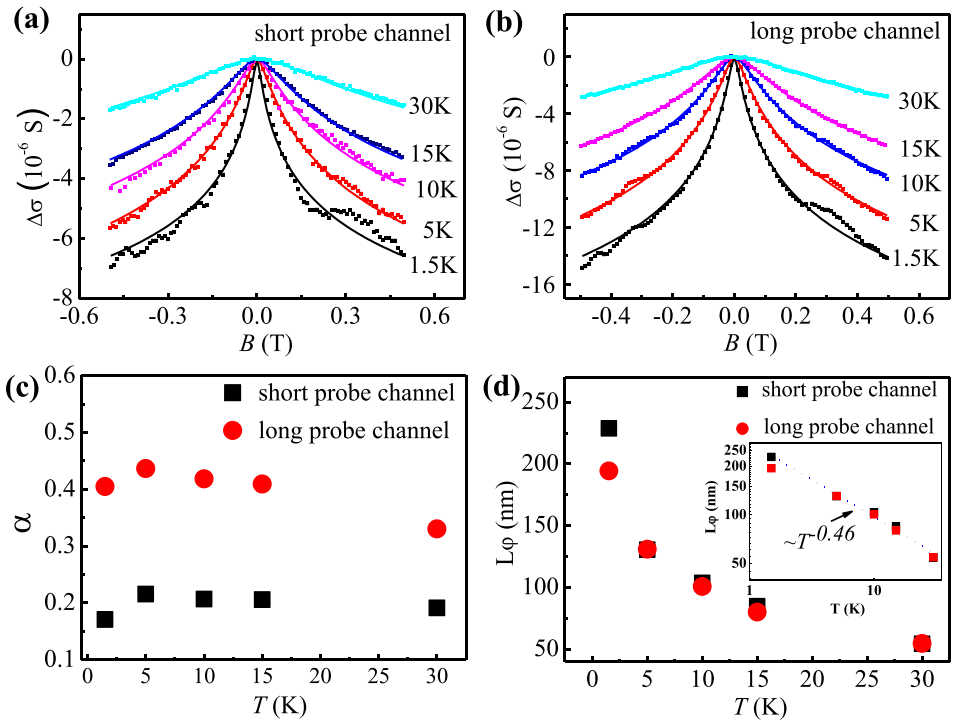

FIG. 3. The conductivity corrections as a function of magnetic field at different temperatures measured in (a) short and (b) long probe channels. The data points fit well with the HLN equation. (c) The temperature dependence of α. (d) The temperature dependence of L_φ. The inset shows the relation $L_\varphi \sim T^{-0.46}$.

One question arises as to that why the α reveals a big reduction but the L_φ is the same for the different probe channels in the same device. The α deviation is often ascribed to the surface-to-bulk coupling in previous reports.[22,23] However, the coupling will lead to extra scattering mechanisms and the observed L_φ should be different in two channels. This indicates that the widely reported surface-to-bulk coupling might not be the dominant mechanism. So far, other physical mechanisms such as the competing effect between topological delocalization and electron-electron interaction have been put forward to account for the quantum correction deviation in the WAL effect.[28,29] However, it is still impossible to explain the observed deviated α and consistent L_φ in short and long probe channels.

The back-gate voltage could tune the Fermi level and thus the surface-to-bulk carrier concentration ratio and also the surface-to-bulk coupling strength.[14,30,31] The magnetoconductance was performed at back-gate voltage ranging from –60 to 60 V, as shown in Figs. 4(a) and 4(b). The extracted α and L_φ are shown in Figs. 4(c) and 4(d), respectively. The results show that α has a weak gate voltage dependence, and it follows the same tendency in two channels. L_φ also does not reveal obvious gate dependence in both channels. Therefore, the surface-to-bulk coupling effect should not be the dominant mechanism

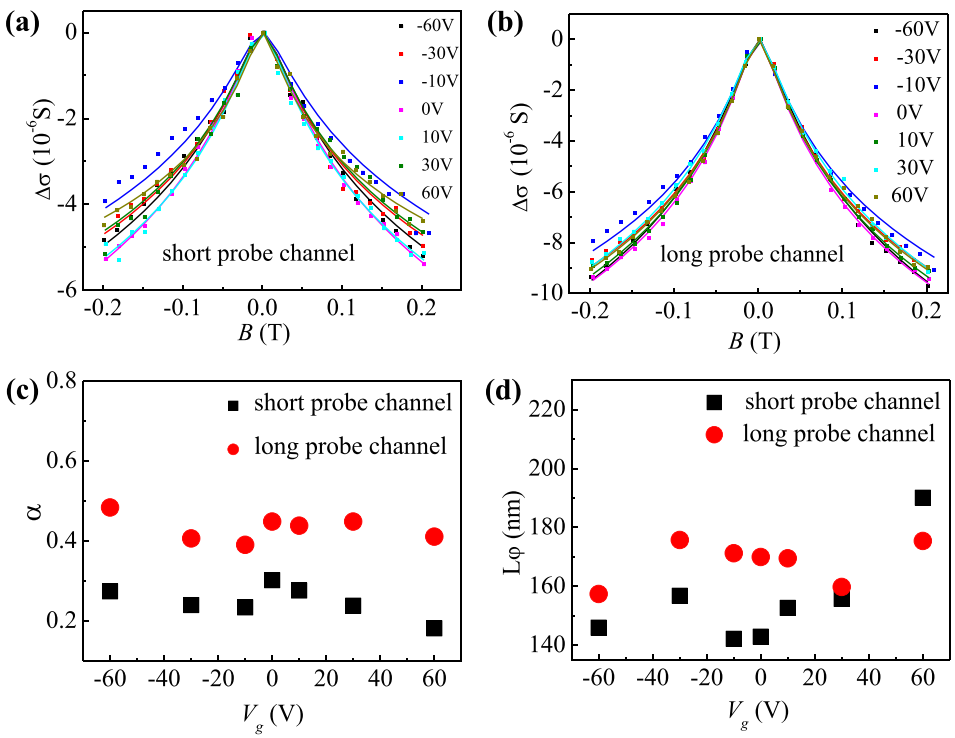

FIG. 4. The conductivity corrections as a function of magnetic field at different gate voltages measured in (a) short and (b) long probe channels at 1.5 K. (c) α and (d) L_φ as a function of gate voltage.

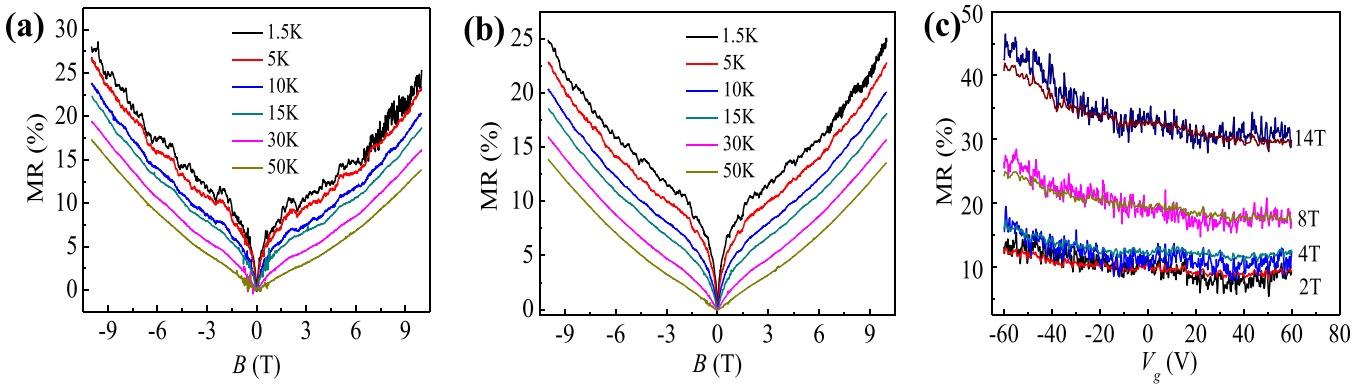

FIG. 5. The MR measured at different temperatures in the (a) short and (b) long probe channels. (c) The MR as a function of gate voltage at different magnetic fields measured from both the short and long probe channels. The MR of the short and long probe channels coincides with each other.

in our transport behaviors. The extracted coherence length is 220 nm and is almost the same as the short probe channel length. Therefore, only partial coherence loops that are smaller than the channel length can contribute to the quantum interference. This leads to a lower conductance correction and a reduced α value. This quantum size-confined effect should be more important in systems with a longer L_φ.

The discussed magnetoconductance reduction is mainly from the quantum interference under low magnetic fields. The non-saturating magnetoresistance (MR) is widely observed in topological insulators up to high magnetic field, and the MR, $[R(B)-R(0)]/R(0)$, is proportional to the carrier mobility.[32–34] As shown in Figs. 5(a) and 5(b), non-saturating MR is the same in both short and long probe channels with the magnetic field up to 10 T. The MR decreases as temperature increases. Figure 5(c) shows the MR as a function of gate voltage. The MR of short and long probe channels well coincides with each other at different gate voltages. These observations support the homogeneous carrier mobility in the short and long probe channels.

In conclusion, the magnetoconductance of a topological insulator BSTS with different channel lengths has been studied. A WAL effect has been observed and the fitted α value in short channel reduces by a factor of 2 compared with that of the long channel. The phase coherence length L_φ is independent of the probe channel length and follows a $T^{-0.5}$ dependence. The gate voltage dependence of α and L_φ indicates that the surface-to-bulk coupling may not be the dominant mechanism for the α reduction. The confined interference path should play an important role in the conductance correction as the L_φ is comparable to the channel length.

This work was supported by the National Key Research and Development Program of China (No. 2016YFA0300802) and NSFC (No. 11774004). S.-M.H. acknowledges the Taiwan National Science Council through Grant Nos. MOST 103-2112-M-110-009-MY3 and MOST 106-2112-M-110-002.

[1]J. Moore, Nat. Phys. **5**, 378 (2009).
[2]S. Y. Xu, Y. Xia, L. A. Wray, S. Jia, F. Meier, J. H. Dil, J. Osterwalder, B. Slomski, A. Bansil, H. Lin *et al.*, Science **332**, 560 (2011).
[3]J. E. Moore, Nature **464**, 194 (2010).
[4]Y. Xia, D. Qian, D. Hsieh, L. Wray, A. Pal, H. Lin, A. Bansil, D. Grauer, Y. S. Hor, R. J. Cava *et al.*, Nat. Phys. **5**, 398 (2009).
[5]Y. L. Chen, J. G. Analytis, J. H. Chu, Z. K. Liu, S. K. Mo, X. L. Qi, H. J. Zhang, D. H. Lu, X. Dai, Z. Fang *et al.*, Science **325**, 178 (2009).
[6]Y. S. Hor, A. Richardella, P. Roushan, Y. Xia, J. G. Checkelsky, A. Yazdani, M. Z. Hasan, N. P. Ong, and R. J. Cava, Phys. Rev. B **79**, 195208 (2009).
[7]C. Shekhar, C. E. ViolBarbosa, B. Yan, S. Ouardi, W. Schnelle, G. H. Fecher, and C. Felser, Phys. Rev. B **90**, 165140 (2014).
[8]H. T. He, G. Wang, T. Zhang, I. K. Sou, G. K. Wong, J. N. Wang, H. Z. Lu, S. Q. Shen, and F. C. Zhang, Phys. Rev. Lett. **106**, 166805 (2011).
[9]J. Chen, X. Y. He, K. H. Wu, Z. Q. Ji, L. Lu, J. R. Shi, J. H. Smet, and Y. Q. Li, Phys. Rev. B **83**, 241304 (2011).
[10]M. Liu, C. Z. Chang, Z. C. Zhang, Y. Zhang, W. Ruan, K. He, L. L. Wang, X. Chen, J. F. Jia, S. C. Zhang *et al.*, Phys. Rev. B **83**, 165440 (2011).
[11]D. Kim, P. Syers, N. P. Butch, J. Paglione, and M. S. Fuhrer, Nat. Commun. **4**, 2040 (2013).
[12]H. Steinberg, J. B. Laloë, V. Fatemi, J. S. Moodera, and P. Jarillo-Herrero, Phys. Rev. B **84**, 233101 (2011).
[13]L. Bao, L. He, N. Meyer, X. Kou, P. Zhang, Z. G. Chen, A. V. Fedorov, J. Zou, T. M. Riedemann, T. A. Lograsso *et al.*, Sci. Rep. **2**, 726 (2012).
[14]J. Lee, J. Park, J.-H. Lee, J. S. Kim, and H.-J. Lee, Phys. Rev. B **86**, 245321 (2012).
[15]S. Matsuo, T. Koyama, K. Shimamura, T. Arakawa, Y. Nishihara, D. Chiba, K. Kobayashi, T. Ono, C. Z. Chang, K. He *et al.*, Phys. Rev. B **85**, 075440 (2012).
[16]B. Xia, P. Ren, A. Sulaev, P. Liu, S. Q. Shen, and L. Wang, Phys. Rev. B **87**, 085442 (2013).
[17]Y. Takagaki, A. Giussani, K. Perumal, R. Calarco, and K. J. Friedland, Phys. Rev. B **86**, 125137 (2012).
[18]S.-P. Chiu and J.-J. Lin, Phys. Rev. B **87**, 035122 (2013).
[19]Y. Xu, I. Miotkowski, C. Liu, J. Tian, H. Nam, N. Alidoust, J. Hu, C. Shih, M. Z. Hasan, and Y. P. Chen, Nat. Phys. **10**, 956 (2014).
[20]A. Kogar, S. Vig, A. Thaler, M. H. Wong, Y. Xiao, I. P. D. Reig, G. Y. Cho, T. Valla, Z. Pan, J. Schneeloch *et al.*, Phys. Rev. Lett. **115**, 257402 (2015).
[21]S. Zhang, L. Pi, R. Wang, G. L. Yu, X. C. Pan, Z. X. Wei, J. L. Zhang, C. Y. Xi, Z. B. Bai, F. C. Fei *et al.*, Nat. Commun. **8**, 977 (2017).
[22]L.-X. Wang, Y. Yan, Z.-M. Liao, and D.-P. Yu, Appl. Phys. Lett. **106**, 063103 (2015).
[23]J. J. Cha, D. Kong, S. S. Hong, J. G. Analytis, K. Lai, and Y. Cui, Nano Lett. **12**, 1107 (2012).
[24]W. Ning, H. Du, F. Kong, J. Yang, Y. Han, M. Tian, and Y. Zhang, Sci. Rep. **3**, 1564 (2013).
[25]K. Banerjee, J. Son, P. Deorani, P. Ren, L. Wang, and H. Yang, Phys. Rev. B **90**, 235427 (2014).
[26]Y. H. Liu, C. W. Chong, J. L. Jheng, S. Y. Huang, J. C. A. Huang, Z. Li, H. Qiu, S. M. Huang, and V. V. Marchenkov, Appl. Phys. Lett. **107**, 012106 (2015).
[27]J. Liao, Y. Ou, X. Feng, S. Yang, C. Lin, W. Yang, K. Wu, K. He, X. Ma, Q. K. Xue *et al.*, Phys. Rev. Lett. **114**, 216601 (2015).
[28]J. Liao, Y. Ou, H. Liu, K. He, X. Ma, Q.-K. Xue, and Y. Li, Nat. Commun. **8**, 16071 (2017).

[29]P. M. Ostrovsky, I. V. Gornyi, and A. D. Mirlin, Phys. Rev. Lett. **105**, 036803 (2010).
[30]J. Chen, H. J. Qin, F. Yang, J. Liu, T. Guan, F. M. Qu, G. H. Zhang, J. R. Shi, X. C. Xie, C. L. Yang *et al*., Phys. Rev. Lett. **105**, 176602 (2010).
[31]F. X. Xiu, L. He, Y. Wang, L. Cheng, L. T. Chang, M. Lang, G. Huang, X. F. Kou, Y. Zhou, X. W. Jiang *et al*., Nat. Nanotechnol. **6**, 216 (2011).
[32]B. A. Assaf, T. Cardinal, P. Wei, F. Katmis, J. S. Moodera, and D. Heiman, Appl. Phys. Lett. **102**, 012102 (2013).
[33]Y. Yan, L. X. Wang, D. P. Yu, and Z. M. Liao, Appl. Phys. Lett. **103**, 033106 (2013).
[34]X. L. Wang, Y. Du, S. X. Dou, and C. Zhang, Phys. Rev. Lett. **108**, 266806 (2012).